LWA-SV Pointing Error and Correction

LWA Memo #206

Jayce Dowell* Savin Varghese†

October 20, 2017

Contents

List of Tables

List of Figures

*University of New Mexico. E-mail: jdowell@unm.edu
†University of New Mexico. E-mail: savin@unm.edu

1 Introduction

This memo documents the determination of the pointing error at LWA-SV and the correction applied in the monitor and control software to minimize the error. A pointing error was first suspected in early 2017 with the first successful pulsar observations with the Advanced Digital Processor (ADP). These observation showed that the sensitivity of LWA-SV was better for sources before transit (rising) than for sources after transit (setting). In addition, the sensitivity of the beam appeared to be better for sources north of the celestial equator. Preliminary analysis of all-sky images from the station revealed a large, $\approx 8^\circ$, rotation in the stand survey coordinate system. Even after correcting for this and re-calibrating the station a small pointing error remained. It should be noted that the presence of a pointing error at LWA-SV is not surprising given the history of pointing at LWA1 [1].

This memo is organized as follows: Section 2 details the observations obtained for the determination of the pointing error while §3 determines the best-fit correction. A brief discussion of the origins of the error, both at LWA-SV and LWA1, is provided in §4.

2 Data

2.1 Driftscans

Driftscan data were initially collected at LWA-SV in order to evaluate the pointing, similar to what was done at LWA1. However, the ADP currently supports only a single dual polarization beam with two 9.8 MHz tunings. Thus, in order to run the three drifts needed to analyze the pointing at a particular location on the sky, three separate days of observations were needed. In order to support this modification to the LWA1 observing procedure the `PointingCheck` utilities[1] were modified to add a new command-line flag for generating LWA-SV-compatible runs. Driftscan observations began in August of 2017 with observations of Cygnus A at elevations of 30° and 60°, both rising as setting, as well as transit. However, due to an active thunderstorm season and an active region on the Sun at this time many of the observations were corrupted. These problems, combined with the additional time to acquire a full set of observations, lead us to abandon this method.

2.2 Basket Weaves

As an alternative to the driftscan method described above we developed a modifed basket weave approach. This approach is based off the source cut or basket weave approach used by higher frequency instruments such as the VLA. The basic idea is that two scans or cuts are made across a source in different directions in order to determine the apparent location of the source. At the frequencies that the LWA stations operate at, however, ionospheric scintillation on $\sim$10 s timescales make this simple approach difficult since the observed power at any location is a combination of the pointing offset from the source's position convolved with the local ionospheric conditions. To help disentangle these two effects we have created a modified basket weave that interleaves the pointing offsets with an ionospheric reference source. By interleaving the offset pointings with a reference pointing it is possible to interpolate between the two reference observations that bracket the offset and obtain an estimate the amount of scintillation at the offset position[2].

For the observations at LWA-SV the basket weave was implemented with two cuts, one in declination and one in right ascension. Both cuts consist of 17 steps that span $\pm 4^\circ$ with a 6 s dwell time. Each

[1] `https://fornax.phys.unm.edu/lwa/trac/browser/trunk/PointingCheck`

[2] This scintillation estimate is for slow scintillation. Fast, <1 s, is naturally accounted for by averaging over the dwell time for each offset.

of these 34 steps in bracketed by an ionospheric reference source with the same 6 s dwell time. For simplicity, the ionospheric reference was chosen to be the "on source" location used for the basket weave. Figure 1 shows frequency-integrated power as a function of time for one such scan while Figure 2 shows the power as a function of position once the ionospheric correction has been applied. In total, there are 69 steps used per pointing check for a total observation time of ≈7 min. This is substantially shorter than the three, 2 hr observations needed by the original driftscan approach and allows many more sources to be observed on a given day.

2.3 LASI-SV

We also used positions for "A team" sources derived from the LWA All-Sky Imager (LASI-SV) running at LWA-SV. LASI-SV is based on the PASI system deployed at LWA1 and described in [3]. Briefly, this systems receives the 100 kHz bandwidth narrowband transient buffer (TBN) stream from ADP, correlates the data, and produces Stokes I and $|V|$ images of the sky. Since the TBN stream provides data from each of the 256 dual polarization dipoles at the station, many sources can be measured at once. Data from LASI-SV were collected at 74.03 MHz on four seperate occasions between 24 Aug 2017 and 7 Sep 2017 (MJD 57990 to 58004). These data contain the positions for Cygnus A, Cassiopeia A, Taurus A, Virgo A, and the Sun determined every 5 s.

3 Pointing Analysis

Basket weave observations were obtained in early October 2017 for 5 sources at 25 positions. The results from the observations are presented in Table 1 with the sky coverage of the observations shown in Figure 3. Following [1] we fit a "rotation about an axis" model to the data. The best-fit rotation was determined to be:

$$\begin{aligned}\theta &= 36.0^\circ;\\ \phi &= 137.6^\circ;\\ \psi &= -1.2^\circ.\end{aligned}$$

Figure 4 compares the pointing error from Table 1 with the results of applying the above correction. Before the correction, the mean pointing error was 0.83 degrees. After correction, the mean pointing error was reduced to 0.16 degrees. Similar to LWA1, the post-correction pointing errors also do not show a strong correlation with elevation. This rotation axis is within ≈12° of the values derived from the LASI-SV data for sources with elevations >30° of:

$$\begin{aligned}\theta_{\text{LASI-SV}} &= 45.7^\circ;\\ \phi_{\text{LASI-SV}} &= 129.3^\circ;\\ \psi_{\text{LASI-SV}} &= -0.8^\circ,\end{aligned}$$

although the amount of rotation, $\psi_{\text{LASI-SV}}$, is about half a degree smaller. It is not clear where this discrepancy comes from, mainly due to the limited information available on the details of the LASI-SV image analysis pipeline. In particular the LASI-SV software allows for a pointing correction to be applied to derived source positions but it is not clear if this is applied in the standard pipeline[3].

These corrections, however, do not represent the correct values to use for LWA-SV. Due to typographically error in the LWA-SV station static MIB initialization file (SSMIF) the data obtained in

[3]Experiments with the different pointing corrections being applied inside LASI-SV suggest that the correction is *not* applied. This result has not be thoroughly tested and should be considered anecdotal.

October 2017 had a pointing correction already applied. Thus, the values presented above represent a "correction to the correction" rather than the correction itself. In the formalism of [1] we use a rotation matrix, $\mathbb{R}$, to transform the raw observing coordinates, $\vec{c}$, into the corrected coordinates $\vec{b}$ through:

$$\vec{b} = \mathbb{R}\vec{c}. \tag{1}$$

If we have already applied an initial rotation matrix, $\mathbb{R}_i$, to $\vec{c}$ we instead have:

$$\vec{b} = \mathbb{R}_c \left(\mathbb{R}_i \vec{c}\right), \tag{2}$$

where $\mathbb{R}_c$ is the rotation matrix derived from the pointing data. To find the final pointing correction we need to find the values for rotation axis and amount that satisfy:

$$\mathbb{R} = \mathbb{R}_c \mathbb{R}_i. \tag{3}$$

Using a simple brute force approach we find that the pointing correction needed for LWA-SV is:

$$\begin{aligned} \theta_{\text{LWA-SV}} &= 27.9^\circ; \\ \phi_{\text{LWA-SV}} &= 122.0^\circ; \\ \psi_{\text{LWA-SV}} &= -0.4^\circ. \end{aligned}$$

This corresponds to an axis approximately 62 degrees above the northwest horizon (azimuth of $\sim$328 degrees). Strangely, neither of the rotation axes derived from the beam formed data yield are consistent at the few degree level with what was found from the LASI-SV data. This suggests that the LASI-SV data is not a suitable replacement for beam formed observations for evaluating the pointing performance of a station[4].

After applying this correction to the SSMIF and re-observing a subset of 12 of the original sources we find that the residual pointing error at LWA-SV has a mean value of 0.31°. This is larger than what was found for LWA1 in [1] but we note that the value appears to be dominated by two observations for Cygnus A and Taurus A at an elevation of 30° and two observations of Hercules A at an elevation of 60°. Excluding these four points (Table 2) decreases the mean residual pointing error to 0.13°.

4 Discussion

The pointing corrections for both LWA1 and LWA-SV are remarkably consistent, both in terms of the orientation of the rotation axis (high above the northwest horizon) and the magnitude of the rotation about that axis. This is interesting in light of the similarities and differences between the two stations. While both stations have a similar layout of the stands, the coaxial cables have different lengths due to differences in how the cables are installed. Furthermore, the outrigger used for calibration is located east of the LWA1 core while it is to the west at LWA-SV. The two stations were also calibrated using wideband all-sky data obtained within ±1 hr window of Cygnus A transit. However, at LWA1 the data consist of wideband transient buffer (TBW) data which contain the full

[4]It is not obvious why this is the case since both the LASI-SV image and the beam formed data are created using the same dipole data, the same geometry, and the same delay model. This could be the result of an astrometry problem, specifically in mapping the centroided source positions from image coordinates back to topocentric or celestial coordinates. Additional work is needed in order to resolve this apparent discrepancy.

bandwidth of the station whereas LWA-SV uses the frequency domain transient buffer on ADP which delivers up to 20 MHz of bandwidth.

Given these comparisons it seems that the pointing error is likely a result of either:

1. A systematic bias that is intrinsic to the construction of the station, such as rotation of the stand survey coordinate system relative to astronomical north;
2. A systematic bias that is intrinsic to the calibration procedure that arises from the dominance of the sky by Cygnus A and Cassiopeia A viewed at a limited set of orientations; or
3. a combination of the two.

It is not clear which of these cases is most likely given the available data from both stations. Having a rotation in the stand survey coordinate system, similar to what initially effected LWA-SV, clearly introduces a rotation. However, this rotation should have an axis that is pointed towards zenith. The fact that the direction of the rotation about the best-fit axis at LWA-SV is opposite that of LWA1 suggests that it may be related to the layout of the station and the locations of the outriggers. One way to test this hypothesis would be to change the data collection time for calibration data, say within ± 1 hr of Cassiopeia A transit, and seeing how the delay solutions change. Another prospect for determining the origin of this pointing problem may be to collect data on non-astronomical sources, e.g., RFI, and use that to verify the calibration. This is similar to the method used by [2] to evaluate the shape of the LWA1 beam.

References

[1] J. Dowell and C. Grimes, "LWA1 Pointing Error and Correction," Ver. 2.0, Long Wavelength Array Memo No. 194, Mar 21, 2013. [online] http://www.phys.unm.edu/∼lwa/memos.

[2] J. F. Helmboldt, "Measurements of the LWA1 Station Beam and Antenna-based Gains using TBW Observations of RFI with Self-calibration", Long Wavelength Array Memo No. 192, undated. [online] http://www.phys.unm.edu/∼lwa/memos.

[3] K. Obenberger et al., " Monitoring the Sky with the Prototype All-Sky Imager on the LWA1", 2015, JAI, 4, 450004

Source Name	UTC Observation Midpoint [YYYY/MM/DD HH:MM:SS]	Azimuth [DDD:MM.SS.S]	Elevation [DD:MM:SS.S]	RA Error [HH:MM:SS.SS]	Dec. Error [DD:MM:SS.S]
CygA	2017/10/02 02:23:37	4:48:43.4	83:15:17.7	-0:01:41.72	-0:29:53.2
CasA	2017/10/02 04:03:13	27:19:03.3	59:28:34.9	-0:02:25.91	-0:34:51.4
CygA	2017/10/02 04:52:18	293:57:56.6	60:27:07.0	-0:00:39.37	-0:11:22.8
CasA	2017/10/02 05:47:17	0:54:56.6	65:09:13.9	-0:01:29.23	-0:32:08.8
CygA	2017/10/02 07:34:17	301:10:55.2	30:22:22.0	-0:00:20.74	0:12:23.2
TauA	2017/10/02 09:52:59	104:49:30.0	59:29:01.7	-0:03:08.28	-0:41:03.2
TauA	2017/10/02 11:57:33	176:41:23.6	77:56:07.9	-0:02:26.27	-0:27:07.9
VirA	2017/10/02 14:45:27	94:55:30.9	29:23:31.7	-0:04:21.89	-0:53:12.6
VirA	2017/10/02 18:52:30	178:01:57.2	68:12:58.1	-0:03:07.59	-0:30:27.0
VirA	2017/10/02 20:21:49	227:18:58.2	60:38:42.1	-0:01:55.27	-0:08:49.3
CygA	2017/10/02 21:09:01	58:21:06.8	29:19:06.0	-0:05:41.41	-0:47:07.1
HerA	2017/10/02 22:46:03	165:19:38.7	60:07:29.3	-0:03:44.26	-0:18:32.3
VirA	2017/10/02 22:59:22	264:08:33.1	30:39:44.5	-0:03:35.18	0:20:47.2
HerA	2017/10/02 23:12:06	178:28:23.9	60:53:24.1	-0:03:45.70	-0:27:02.4
HerA	2017/10/02 23:38:09	191:43:55.7	60:24:25.0	-0:03:54.63	-0:28:10.5
CasA	2017/10/02 23:53:23	36:20:21.8	29:24:49.5	-0:08:50.09	-0:39:42.1
CasA	2017/10/03 07:27:25	333:44:16.8	60:01:58.5	-0:00:33.05	-0:19:51.0
TauA	2017/10/03 14:50:23	264:07:52.1	50:02:19.6	-0:01:54.61	0:03:15.8
HydA	2017/10/03 14:59:53	166:46:31.6	42:48:56.7	-0:04:43.67	-0:33:05.5
TauA	2017/10/03 15:38:44	271:20:12.2	40:00:44.2	-0:02:53.78	0:16:31.3
VirA	2017/10/03 16:24:00	113:55:24.2	49:58:36.8	-0:03:35.97	-0:43:12.6

Table 1: List of Drift Scan Sets used to Determine the Pointing Error

Source Name	UTC Observation Midpoint [YYYY/MM/DD HH:MM:SS]	Azimuth [DDD:MM.SS.S]	Elevation [DD:MM:SS.S]	RA Error [HH:MM:SS.SS]	Dec. Error [DD:MM:SS.S]
VirA	2017/10/03 20:17:53	227:18:55.7	60:38:42.9	0:00:07.40	0:00:54.5
VirA	2017/10/03 22:55:26	264:08:32.2	30:39:45.7	0:00:27.06	-0:09:32.4
HerA	2017/10/03 23:34:13	191:43:53.3	60:24:25.1	-0:00:24.68	0:00:15.0
CygA	2017/10/03 23:47:04	66:03:48.6	59:19:21.2	0:00:42.39	0:05:29.9
CygA	2017/10/04 02:15:45	4:48:56.6	83:15:17.4	0:00:10.01	0:01:13.8
CasA	2017/10/04 03:09:44	33:33:00.3	54:38:33.8	-0:00:34.14	0:07:46.8
CygA	2017/10/04 04:44:26	293:57:56.8	60:27:08.6	0:00:15.78	-0:07:08.8
TauA	2017/10/04 15:04:51	267:02:38.1	46:13:47.9	0:00:54.57	0:02:29.4

Table 2: List of Drift Scan Sets used to Verify the Pointing Error Correction

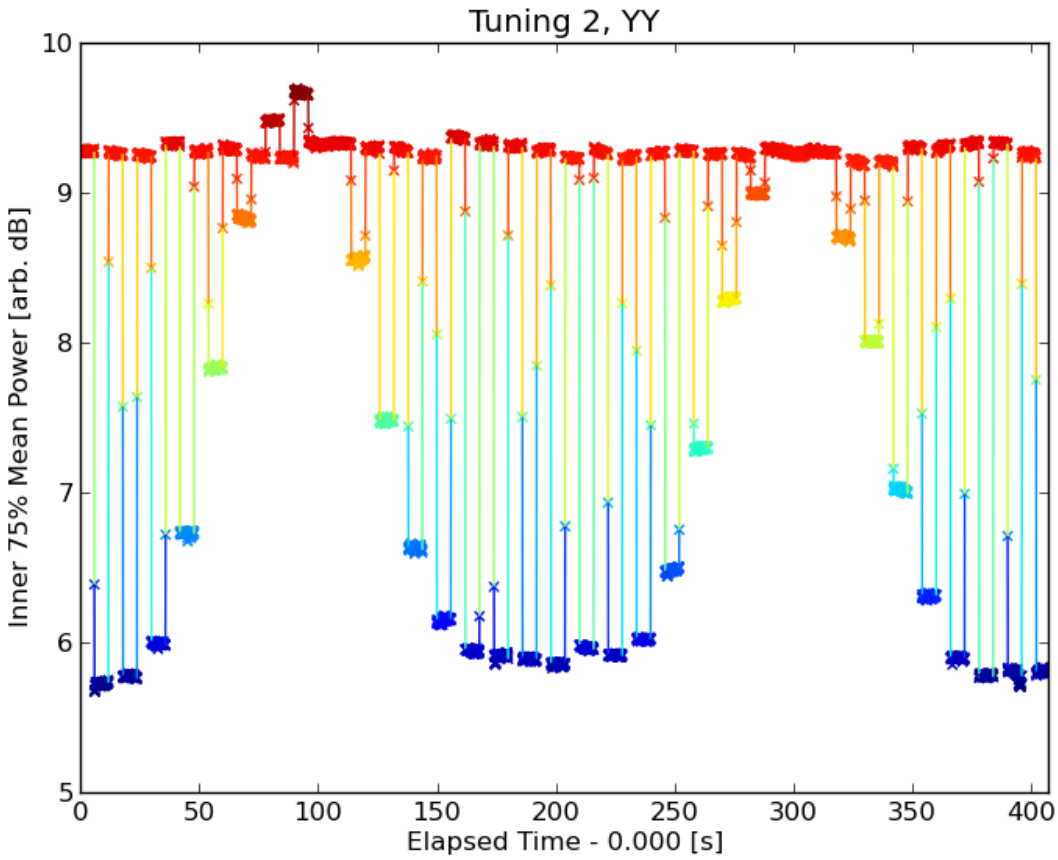

Figure 1: Plot of the driftcurve data (frequency-integrated power as a function of time) from a Cassiopeia A run on 2 Oct 2017 at an elevation of 60°. The x-axis is elapsed time while the y-axis is power. The drfitcurve consists of two families of data. The higher points near ∼9 dB are the ionospheric reference positions which the lower/more variables values are the position offsets. The first set of offsets cut through the source in declination while the second set cut in right ascension. The two cuts converge with the reference data at the source's expected position 1/4 and 3/4 through the observation.

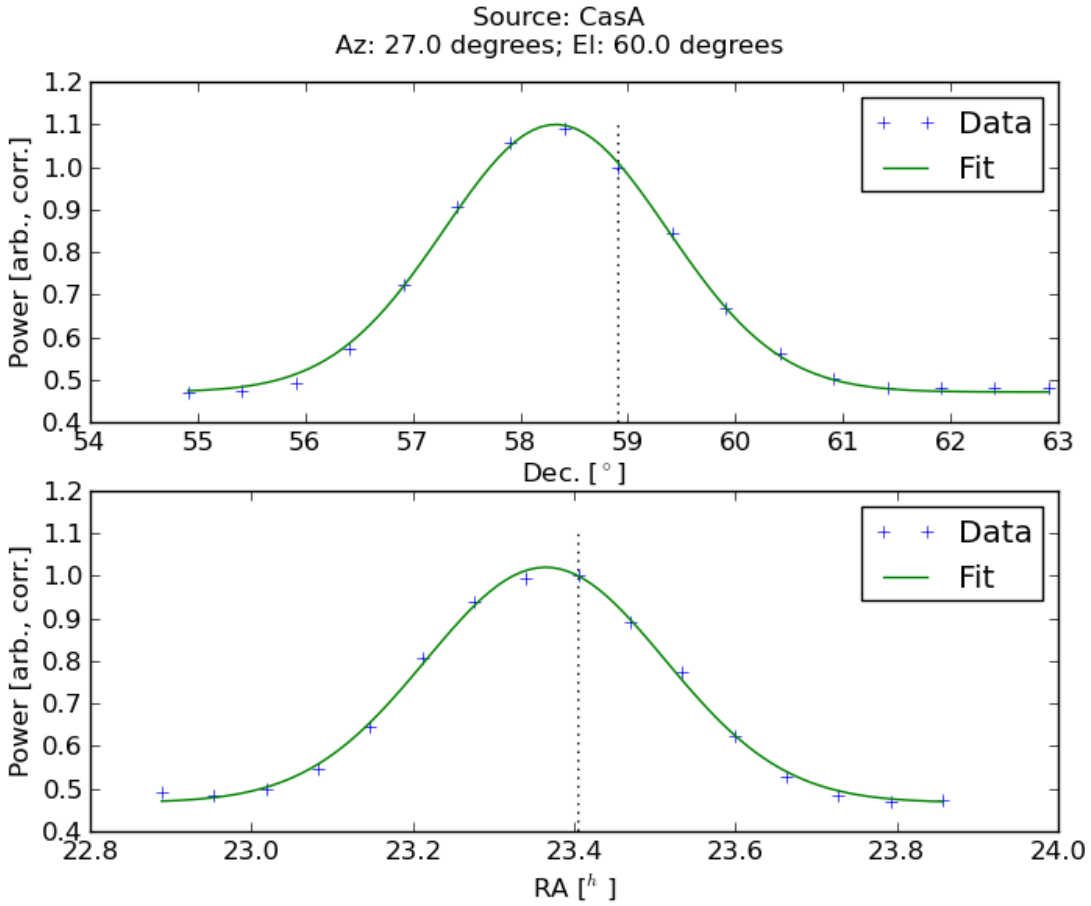

Figure 2: Processed version of the Cassiopeia A run shown in Figure 1. To create this figure the raw driftcurve was first divided into pieces using the pointing information contained in the metadata and then split into its three constituent parts: ionospheric reference, declination cut, and right ascension cut. The ionospheric reference data were then used to create a linear interpolation function that was used to correct the two cuts. The corrected cuts are shown for declination (top) and right ascension (bottom) along with the expected source position (vertical dashed lines).

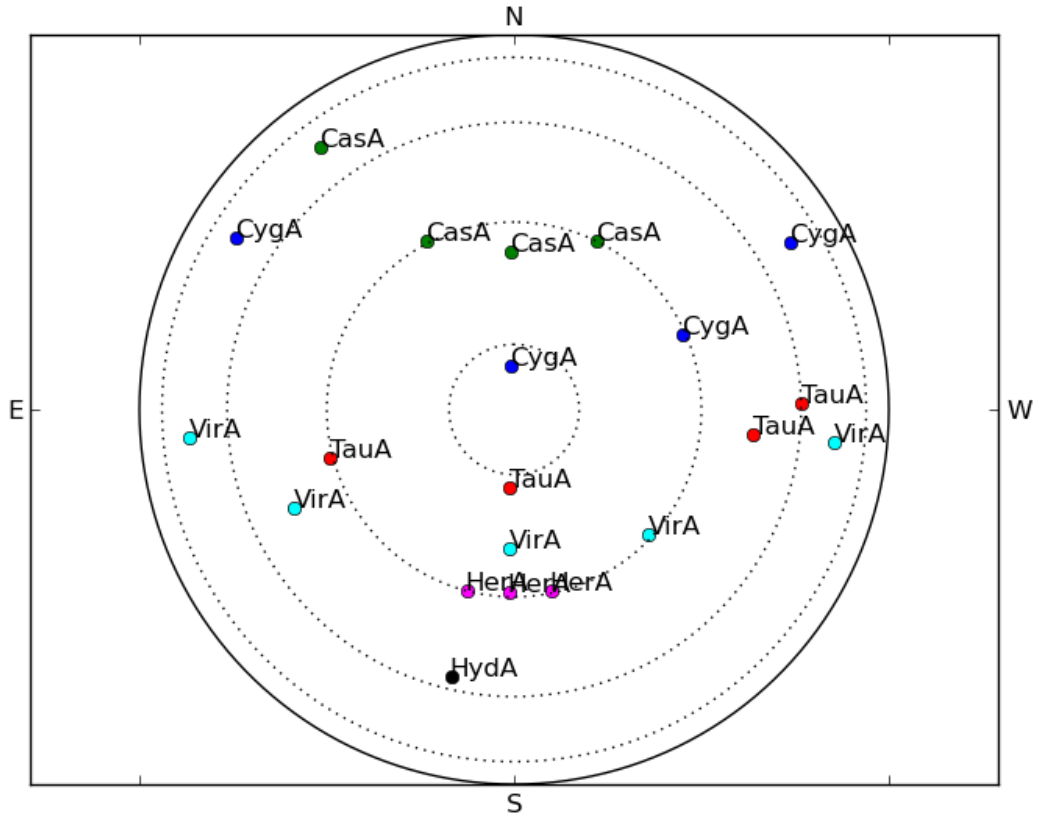

Figure 3: On-sky distribution for the sources listed in Table 1. North is up and east is to the left. Lines of constant elevation are marked by dotted lines at 20°, 40°, 60°, and 80°.

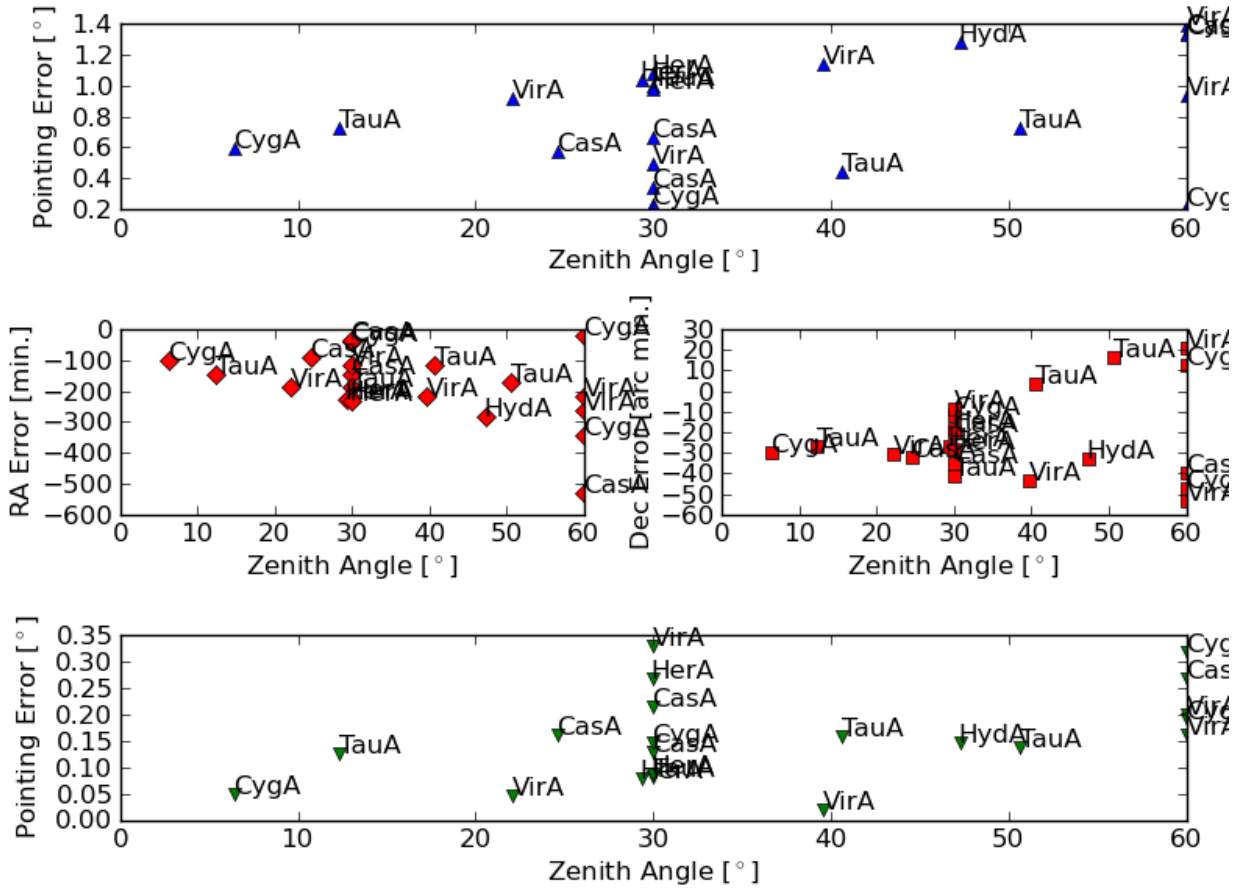

Figure 4: Comparison between the raw pointing offsets (total – top panel; by RA and Dec. – middle two panels) and the corrected pointing offsets (bottom panel). The source associated with each data point is listed to the upper right. Before correction the mean pointing error is ∼0.8°and the mean error is ∼0.2°after correction.